JOURNAL OF VIROLOGY, Jan. 1991, p. 7–15
0022-538X/91/010007-09$02.00/0

Vol. 65, No. 1

Identification of a Common Viral Integration Region in Cas-Br-E Murine Leukemia Virus-Induced Non-T-, Non-B-Cell Lymphomas

DOMINIQUE BERGERON,[1] LAURENT POLIQUIN,[1] CHRISTINE A. KOZAK,[2] AND ERIC RASSART[1]*

Département des Sciences Biologiques, Université du Québec à Montréal, C. P. 8888 Succursale A, Montréal H3C 3P8, Canada,[1] and Laboratory of Molecular Microbiology, National Institutes of Health, Bethesda, Maryland 20892[2]

Received 10 April 1990/Accepted 28 September 1990

The Cas-Br-E murine leukemia virus is a nondefective retrovirus that induces non-T-, non-B-cell lymphomas in susceptible NIH/Swiss mice. By using a DNA probe derived from Cas-Br-E provirus-flanking sequences, we identified a DNA region, originally called *Sic-1*, rearranged in 16 of 24 tumors analyzed (67%). All proviruses were integrated in a DNA segment smaller than 100 bp and were in the same 5′-to-3′ orientation. Ecotropic as well as mink cell focus-forming virus types were found integrated in that specific DNA region. On the basis of Southern blot analysis of somatic cell hybrids and progeny of an interspecies backcross, the *Sic-1* region was localized on mouse chromosome 9 near the previously described proto-oncogenes or common viral integration sites: *Ets-1*, *Cbl-2*, *Tpl-1*, and *Fli-1*. Restriction map analysis shows that this region is identical to the *Fli-1* locus identified in Friend murine leukemia virus-induced erythroleukemia cell lines and thus may contain sequences also responsible for the development of mouse non-T-, non-B-cell lymphomas.

Studies on the mechanism of tumorigenicity by nonacute retroviruses have shown that cellular transformation induced by these viruses could be due to insertional mutagenesis. A search for common sites of proviral integration in tumor DNA is therefore useful to identify new cellular proto-oncogenes. Such an experimental approach has been fruitful in identifying proto-oncogenes or potential proto-oncogenes in murine tumors such as *Int-1*, *Int-2*, *Int-3*, and *Int-41* in mouse mammary tumor virus-induced mammary carcinomas (13, 14, 38, 40); N-*myc*, *Myc*, *Pim-1*, *Pim-2*, *Mlvi-1*/*Mis-1*/*Pvt-1*, *Mlvi-2*, *Gin-1*, *Dsi-1*, *Fis-1*, *Tpl-1*, and H-*ras-1* predominantly in T-cell lymphomas (2, 4, 8–10, 24, 28, 32, 58, 60, 62) and *Myb*, *Evi-1*/*Fim-3*, *Fim-1*, *Fim-2*/*Csfmr*, and *Fis-1* in myelogenous leukemias (17, 32, 52, 54, 56) induced by a variety of murine leukemia viruses (MuLVs); *Fli-1* in Friend MuLV and *Spi-1* in spleen focus-forming virus-induced erythroleukemia (3, 30) and finally *Ahi-1* in pre-B lymphomas induced by helper Moloney MuLV in Abelson murine infection (42). Although by no means exhaustive, this enumeration suggests that sites of tumor-associated integrations have some specificity for distinctive tumor types.

The Cas-Br-E (referred to as Cas-Br-M in some studies) MuLV is an ecotropic nondefective retrovirus that induces a progressive form of hind-limb paralysis and leukemia after inoculation into susceptible mice (15, 20). Cas-Br-E MuLV is somewhat unusual in that it can induce a wide spectrum of hematopoietic neoplasms in NFS/N mice, including T-pre-B- and B-cell lymphomas, erythroleukemias, and myelogenous and megakaryocytic leukemias (12, 23). Biologically cloned mink cell focus-forming recombinant virus (MCF) isolated from Cas-Br-E-induced thymic lymphoma caused almost exclusively thymic or nonthymic T-cell lymphomas in NFS mice (7, 21). However, the type of neoplasm induced also depends on the strain of mouse inoculated, since it has been reported that only non-T-, non-B-cell lymphomas were observed after inoculation of NIH/Swiss mice with Cas-Br-E MuLV (5). Viral integrations of Cas-Br-E MuLV in cell lines derived from NFS/N primary myelogenous leukemias or erythroleukemias were frequently detected in the *Evi-1* (33) and *Myb* loci (65). Infectious viruses obtained from a molecular clone of Cas-Br-E MuLV (NE-8) retained the paralysis-inducing and leukemogenic potential of the parental MuLV in NIH/Swiss mice (26). The unusual type of tumors obtained in NIH/Swiss mice (non-T-, non-B-cell lymphoma) prompted us to search for new common provirus integration sites. Therefore, by using a U_3 long terminal repeat (LTR) probe specific for Cas-Br-E MuLV (46), we cloned the proviruses from one tumor, derived probes from the flanking cellular sequences, and screened other tumor DNAs for alterations in the same region of cellular DNA.

We report here that in 67% of the tumors analyzed, parental ecotropic or MCF-like recombinant Cas-Br-E MuLVs were integrated in the same 5′-to-3′ orientation within a very small region of DNA (less than 100 bp). This common integration region has been localized on mouse chromosome 9 and is identical to the *Fli-1* region already described in Friend MuLV-induced erythroleukemias (3).

MATERIALS AND METHODS

Mice, viruses, and tumor pathology. Outbred NIH/Swiss mice were originally purchased from the NIH (Bethesda, Md.) resource facilities and kept in our breeding colony. For induction of lymphomas, newborn (<48 h old) mice were inoculated intraperitoneally with 0.15 ml of filtered (pore size, 0.22 μm; Nuclepore Corp., Pleasanton, Calif.) tissue culture medium containing 10^5 PFU/ml of a molecular clone of Cas-Br-E MuLV (NE-8; 26). Lymphomas developed 3 to 6 months postinoculation, and mice were sacrificed when obvious spleen enlargement was detected by palpation. Diagnoses were based on gross pathology, Wright-Giemsa staining, and microscopic examination of blood smears, tumor imprints, and fixed tissues, according to previously described criteria (39). Progeny from the backcross (NFS/N

* Corresponding author.

× *Mus mus musculus* [Skivel]) (F_1) × *Mus m. musculus* [Skivel]) were generated at NIH.

Southern blot analysis. High-molecular-weight cellular DNA extracted from mouse tissues was digested with appropriate restriction endonucleases, separated by horizontal agarose gel electrophoresis, and transferred to nylon membranes by standard techniques. Specific DNA fragments were detected by hybridization with appropriate ^{32}P-labeled DNA probes. Nylon filters were hybridized in 50% formamide–10% dextran sulfate–6× SSC (1× SSC is 0.15 M NaCl plus 0.015 M sodium citrate)–0.5% sodium dodecyl sulfate (SDS)–5× Denhardt solution at 42°C. After hybridization, the filters were washed sequentially in 2× SSC–0.1% SDS three times for 5 min each at 22°C, in 2× SSC– 0.1% SDS for 30 min at 65°C, and in 0.1× SSC–0.1% SDS at 65°C for 10 min. Wet membranes were exposed at −70°C to X-Omat AR film (Eastman Kodak Co., Rochester, N.Y.) by using a Cronex Lightning-Plus intensifying screen (Du Pont Co., Wilmington, Del.).

Molecular cloning procedures. DNA from tumor 106-2 was digested with *Eco*RI and centrifuged on a sucrose density gradient (10 to 30%) as previously described (45). DNA fragments from 9 to 20 kbp were pooled and ligated to *Eco*RI-cleaved lambda-Dash vector. Smaller DNA fragments were ligated to *Eco*RI-cleaved lambda-gt10 vector. The ligation mixtures were packaged in vitro with Gigapack, according to the manufacturer's instructions (Stratagene, La Jolla, Calif.). The MuLV recombinant bacteriophages were identified with a ^{32}P-labeled Cas-Br-E U_3 LTR-specific probe described previously (46). Subcloning of DNA fragments into pBluescript or pGEM vectors was done according to standard procedures. Labeling of probes was done on purified DNA fragments by the random primer extension method with oligohexamers (Pharmacia, P-L Biochemicals, Montréal, Québec, Canada) (11).

Probes. The immunoglobulin heavy chain region was analyzed with a 6.2-kbp *Eco*RI germ line J_H DNA fragment (1). The murine β-chain T-cell-receptor (TcR) gene was analyzed with a 700-bp RBL5-17 DNA fragment containing most of the murine $C_{\beta 1}$ coding and 3′ untranslated sequence (6). The Cas-Br-E U_3 LTR-specific probe consists of a 280-bp *Stu*I-*Sac*I fragment subcloned in Sp64 plasmid (46). The cellular fragments, free of repetitive sequences, SU9, SU10, and SU11, are respectively an 800-bp *Hin*cII fragment, a 1.1-kbp *Bam*HI-*Hin*cII fragment, and a 1.8-kbp *Eco*RI fragment cloned in pBluescript vector. The *Tpl-1* probe (pSB-1) (2) and the *Ets-1* (exon IX) were kindly provided by Philip Tsichlis (Fox Chase Cancer Center, Philadelphia, Pa.), and the *Fli-1* probe (B2) (3) was kindly provided by Alan Bernstein (Mount Sinai Hospital Research Institute, Toronto, Ontario, Canada).

Somatic cell hybrids. Hybrids used in the chromosomal localization analysis were produced by fusion of Chinese hamster cell line E36 with the cells of inbred mice (22).

RESULTS

Tumor pathology and molecular analysis of immunoglobulin heavy chain and TcR β-chain genes. Newborn NIH/Swiss mice from 12 litters (97 mice) were inoculated with the NE-8 molecular clone of Cas-Br-E MuLV (26). Over the next 3 to 5 months, 59 mice developed splenomegaly as detected by palpation and were sacrificed for histopathology and molecular analysis studies of their tissues. During the same period, some mice developed neurological disease. Tumors obtained from an earlier experiment (seven spleen tumors of 11 NIH/Swiss newborn mice injected) were also included in our study (tumor numbers 105-1, 105-2, 106-1, 106-2, 106-3, and 106-4). In these cases, the latency was longer (from 7 to 12 months), possibly due to virus titer variations. Nevertheless, all these NE-8 Cas-Br-E-induced lymphomas still showed very comparable pathological characteristics: they arose primarily in the spleen, spared the thymus, and occasionally became leukemic, invading other organs (kidneys and liver). Most tumor cells were monomorphic undifferentiated lymphoblastoid cells with high nuclear-to-cytoplasmic ratios. The large round nuclei contained distinct nucleoli and dispersed chromatin.

Rearrangements within immunoglobulin and TcR genes, which normally occur during B-cell and T-cell differentiation, respectively, can serve as convenient diagnostic markers for determining the cell lineage involved in the development of given lymphomas. Analysis of immunoglobulin heavy chain genes was performed on *Eco*RI-digested tumor DNAs with a J_H-specific probe (1). The TcR β region was examined with a $C_{\beta 1}$ probe on *Hin*dIII-digested DNAs (6). No detectable rearrangements were observed for these loci in 23 of the 25 tumor DNAs analyzed (Fig. 1). A faint rearranged fragment could be seen in tumor 106-1 (Fig. 1A, lane 15). This tumor, which appears clonal on the basis of the analysis presented in the next sections, may contain a subpopulation derived from a clone of pre-B or B cells. Whether these stem from differentiation of a tumor cell remains to be seen. The one tumor for which a clear rearrangement could be detected with the TcR β probe, tumor 45 (Fig. 1B, lane 3), was also the only one to show enlargement of the thymus and the lymph nodes in addition to that of the spleen and was thus classified as a T-cell lymphoma. Note that, as already reported (42), the TcR β-chain locus shows polymorphism in outbred NIH/Swiss mice, as demonstrated by the two fragments at 9.4 and 9.2 kbp (Fig. 1B).

To summarize, NE-8 Cas-Br-E-induced tumors were classified as non-T-, non-B-cell lymphomas probably of stem cell origin, on the basis of germ line configuration at the immunoglobulin heavy chain region and TcR β-chain loci and of histopathological analyses which indicated that the tumor cells appear to belong to the lymphoid lineage. Taken together, these data show that the disease induced in NIH/Swiss mice by the molecular clone of Cas-Br-E is identical to that described by Bryant et al. (5) following infection of NIH/Swiss mice with a biological clone of Cas-Br-E virus, as well as lymphomas observed in Lake Casitas wild mice from which Cas-Br-E was originally isolated (5, 16).

Characterization of genomic DNAs from independent tumors and cloning of integration sites from one tumor. As a first step to further characterize integration events having taken place during the development of tumors, genomic DNA was purified from 24 independently obtained lymphomas and analyzed by Southern transfer following *Eco*RI digestion, by using a probe specific for the U_3 region of the Cas-Br-E LTR (46). Figure 2 shows the result for a subset of the lymphomas analyzed. The probe does not detect any endogenous NIH sequences (Fig. 2, lane 1) and therefore allows one to identify newly acquired proviral sequences in Cas-Br-E-induced tumors. All of these lymphomas appear to be of clonal origin since they contain a discrete set of newly acquired fragments (Fig. 2, lanes 2 to 10). Each tumor also shows a unique hybridization pattern, which is to be expected for independent infection events.

In order to test whether any integration site was frequently associated with tumors, we cloned all the newly acquired

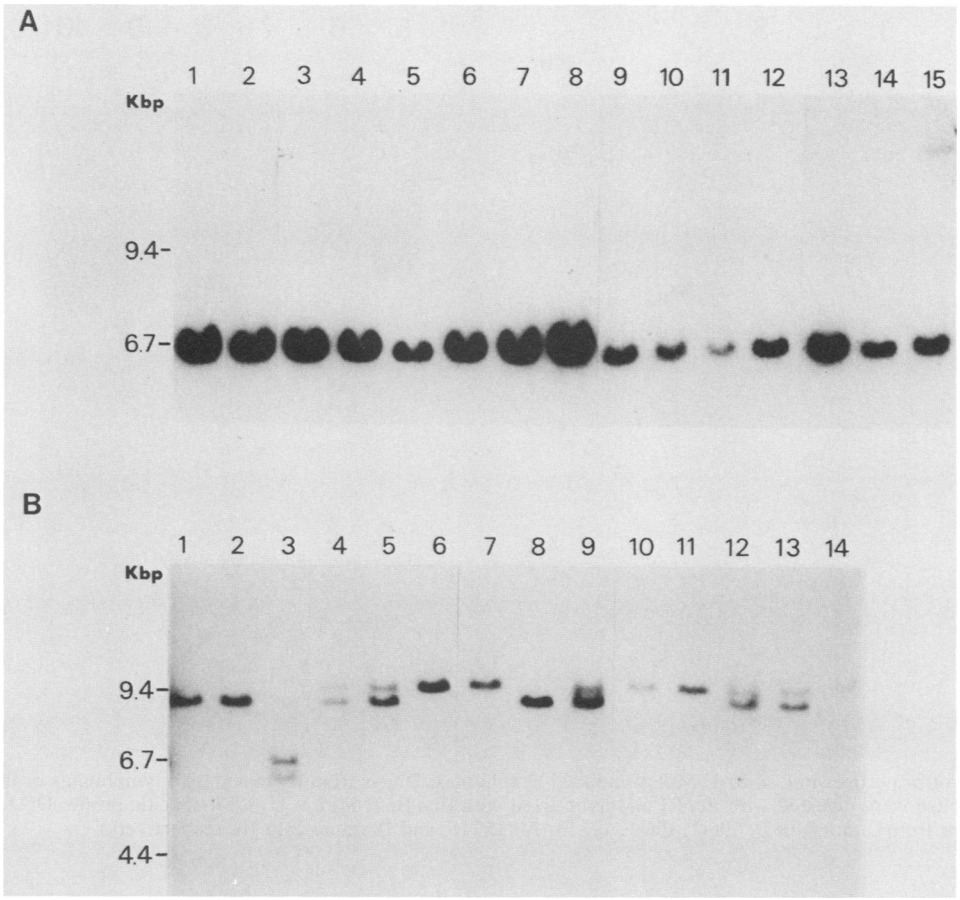

FIG. 1. Southern blot analysis of the immunoglobulin heavy chain and the T-cell-receptor β-chain loci in Cas-Br-E-induced lymphomas. DNAs were digested with *Eco*RI (A) or *Hin*dIII (B) and hybridized with probes specific for J_H and the TcR β-chain constant region ($C_{\beta 1}$), respectively. (A) DNAs from the liver of a normal NIH/Swiss mouse (lane 1) or from Cas-Br-E MuLV induced from lymphomas 45, 12, 13, 14, 15, 16, 18, 5, 106-4, 105-2, 105-1, 106-3, 106-2, 106-1 (lanes 2 to 15, respectively); (B) control DNAs from the normal liver of a NIH/Swiss mouse (lane 1) or from the kidney of a mouse with tumor 5 (lane 2) and DNAs from Cas-Br-E MuLV-induced lymphomas 45, 14, 13, 12, 6, 5, 4, 106-3, 106-2, 105-2, 105-1, and 106-4 (lanes 3 to 14, respectively).

viral integrations from one tumor. Tumor 106-2 was chosen for this purpose because of its less complex integration pattern (Fig. 2, lane 3). Tumor DNA was digested with *Eco*RI and inserted into lambda vectors, and recombinant clones containing Cas-Br-E proviruses were identified by hybridization with the U_3-specific Cas-Br-E LTR probe. All five of the proviruses detectable in tumor 106-2 DNA were successfully cloned. Four clones were shown by restriction map analysis to represent full-length ecotropic NE-8 Cas-Br-E integrations with their flanking cellular sequences. They comigrated with the four DNA bands larger than 9.4 kbp in the original tumor (data not shown). At least one of these proviruses is nondefective, since infectious virus was recovered after transfection on NIH 3T3 cells. DNA probes were derived from unique regions in the adjacent cellular sequences for each of these four clones; they failed to detect rearrangement in any of the 24 lymphomas analyzed.

A fifth clone, labeled gtBib, is a 6.0-kbp *Eco*RI fragment corresponding to the 6-kbp band seen in Fig. 2, lane 3. It represents the 3′ end of an MCF-like recombinant provirus with 3′-adjacent cellular sequences (4 kbp from the insertion site to the *Eco*RI site downstream [see Fig. 4]). Indeed, this clone harbors Cas-Br-E LTR sequences as demonstrated by hybridization to the U_3-specific probe and shows an *Eco*RI site at position 6.9 of the proviral genome, typical of MCF proviruses (43). The possibility that the corresponding 5′ region of the proviral genome was lost in tumor 106-2 has to be considered because (i) all the fragments detectable by Southern hybridization with the Cas-Br-E U_3 probe were cloned, each in several copies, making it unlikely that an incomplete library was screened (upon restriction analysis, none of these corresponded to the 5′ portion of the MCF integration) and (ii) the 5′ LTR portion of the MCF provirus should be included in an *Eco*RI fragment, which we do not detect in the Southern blot.

Detection of frequent rearrangements in a specific genomic region. Probes corresponding to cellular sequences adjacent to the MCF-like gtBib provirus were derived (see Fig. 4, segments SU9, SU10, and SU11). When these probes were used on DNAs from Cas-Br-E-induced lymphomas, 67% (16 of 24) of the tumors showed rearrangement in that region with at least four different restriction endonucleases. Southern transfers performed with *Eco*RI, *Sac*I, and *Pst*I digests are shown in Fig. 3 for a subset of the analyzed lymphoma DNAs. In each tumor, the configuration of altered cleavage sites fits precisely with what would be predicted either for an

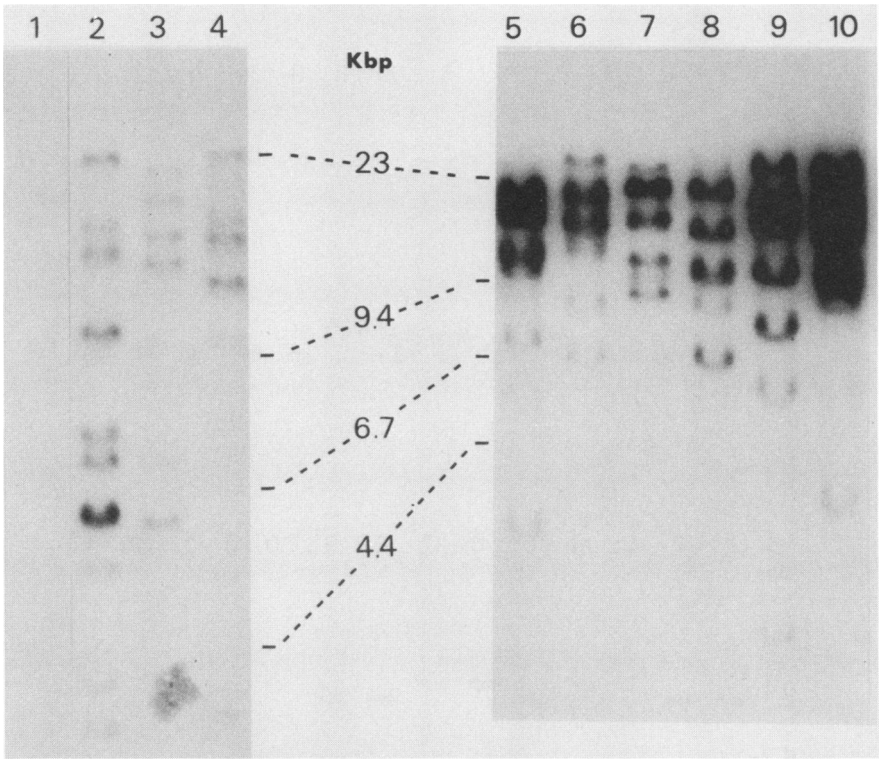

FIG. 2. Analysis of proviruses in Cas-Br-E MuLV-induced lymphomas. DNAs from representative lymphomas or from the normal liver of an NIH/Swiss mouse were digested with *Eco*RI and hybridized with Cas-Br-E MuLV U_3-LTR-specific probe. DNAs were from normal liver DNA (lane 1) or from tumors 106-3, 106-2, 106-1, 12, 13, 14, 15, 16, and 18 (lanes 2 to 10, respectively).

ecotropic or MCF-like viral insertion. In all cases, the nonrearranged allele was also detected. Since the NIH/Swiss line is outbred and rearrangements produced remarkably similar fragments, polymorphism had to be considered. This possibility was excluded by comparing DNAs from normal tissues of tumor-harboring animals to their tumor counterparts. The rearranged fragment is absent from brain (Fig. 3B, lane 15) and kidney (lane 13), but present in tumor tissue from the same animals (lanes 14 and 12, respectively). Faint rearranged fragments were detectable in kidney DNAs from some animals, probably due to infiltration of leukemic cells (data not shown). Rearranged and normal alleles appeared to be equimolar in all tumors, as evidenced by their comparable intensities of hybridization, thus confirming that most, if not all, cells in a tumor show the same rearrangement and suggesting the clonal origin of the tumors. This frequently rearranged chromosomal region is referred to as *Sic-1* (site d'intégration de Cas-Br-E). (We reported part of our results, by using the *Sic-1* name, at the RNA Tumor Viruses meeting [Cold Spring Harbor, May 1990] and at the Oncogenes meeting [Bethesda, June 1990]. Since we now know that *Sic-1* is identical to *Fli-1*, we suggest that *Fli-1* be kept for identifying the chromosomal locus).

Structural organization of proviruses in the *Sic-1* region. The *Sic-1* region of normal NIH/Swiss mouse DNA was further characterized by restriction enzyme digestions and Southern analysis with the SU9 or SU10 probes (Fig. 4). The general organization of proviral insertions was also determined by performing the same analysis on tumor DNAs (Fig. 3 and data not shown). The results are summarized in Table 1 and Fig. 4. Identification of MCF versus ecotropic integrations was made with the *Eco*RI digestion, making use of the *Eco*RI site typically found in the *env* region of MCF recombinants (position 6.9 of their genome) and of its absence in ecotropic viruses. Thus, 10 tumor DNAs showed a 13.8-kbp *Eco*RI fragment which hybridizes to SU10 (Fig. 3A, lanes 2, 3, 5, and 6), corresponding to the insertion of an *Eco*RI-free full-length ecotropic genome in the 5.0-kbp fragment of the normal allele (lane 1). Another four tumors showed a smaller, rearranged *Eco*RI fragment, revealing the presence of the *Eco*RI site typical of MCF recombinants (lanes 4, 8, and 9). These also show some differences elsewhere in their genomes (Table 1 and data not shown), as expected for recombination events involving different endogenous sequences. The MCF-like recombinants found in the *Sic-1* region have acquired a new *env* gene (as shown by the presence of the *Eco*RI site) but, on the basis of hybridization with a specific U_3-LTR probe, they seem to have retained the LTR from the inoculated ecotropic MuLV. Attempts to further characterize the 5′ portion of the MCF-like insertions await the isolation of cellular probes from regions upstream of the integration site. Finally, one tumor (Table 1, tumor 13) clearly showed *Eco*RI fragments characteristic of both ecotropic and MCF recombinant insertions (data not shown). This tumor may contain a mixed population of tumor cells, one part arising after an ecotropic insertion and the other part after an MCF insertion, with both types conferring equal growth advantages. Although unusual, this may not be totally unexpected in view of the high frequency of integration at the *Sic-1* locus. This phenomenon is still under investigation.

More precise localization of the proviral insertions in the *Sic-1* region was determined by analysis of *Sac*I-digested tumor DNAs hybridized to SU10. The Cas-Br-E genome

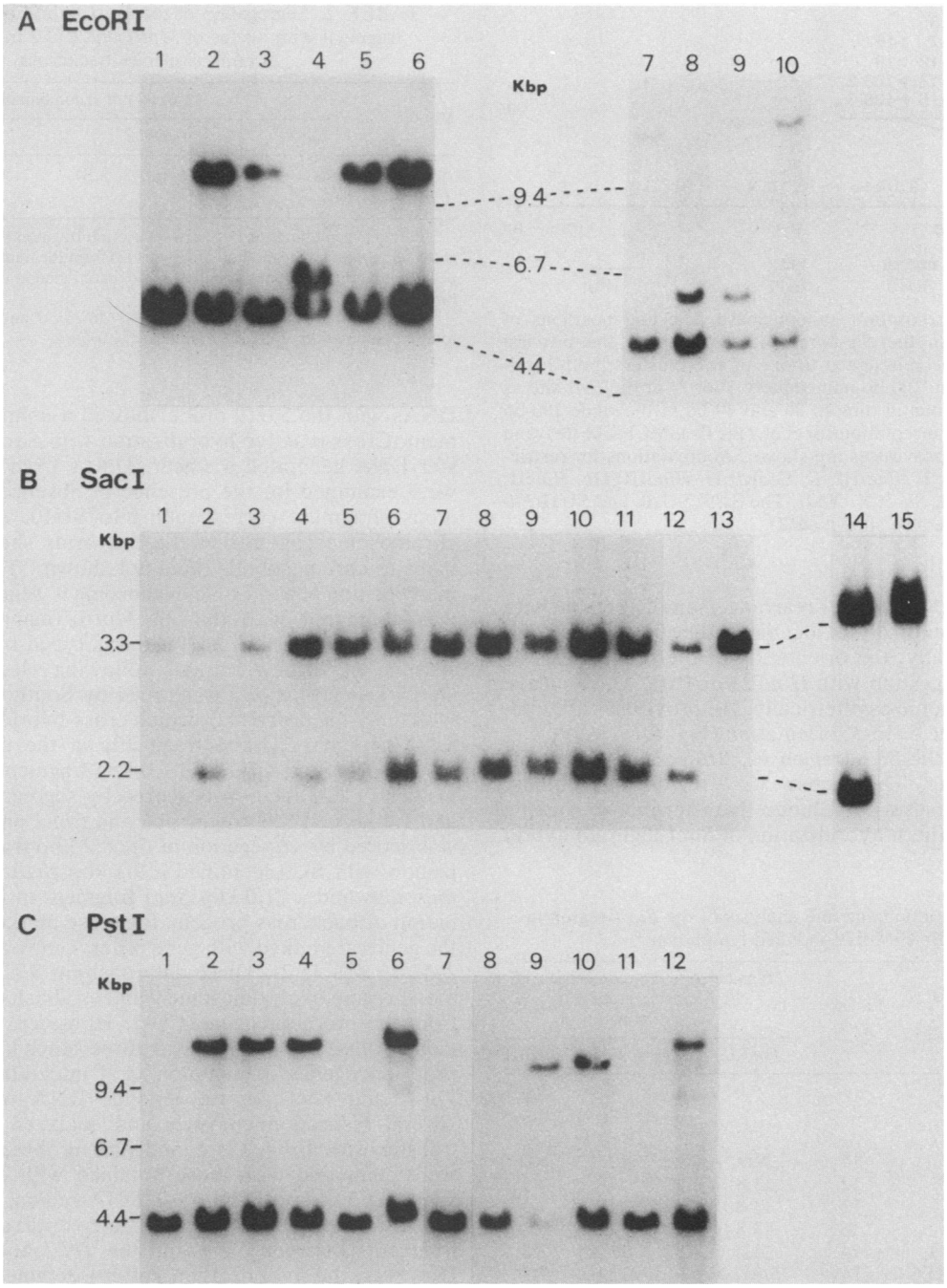

FIG. 3. Identification of a common site of viral integration by Southern blot analysis. Cas-Br-E tumor DNAs were digested with the indicated restriction enzyme and hybridized to SU10 probe. (A) DNAs from tumors 12, 14, 15, 16, 18, 105-1, 106-3, 106-2, and 106-1 (lanes 2 to 10, respectively). (B) DNAs from tumors 106-1, 106-2, 106-3, 105-1, 4, 12, 14, 15, 16, and 18 (lanes 2 to 11, respectively). Lanes 12 to 15 show pairs of DNAs from tumor tissues and control organs from the same animal (tumor 5 and the corresponding kidney [lanes 12 and 13] and tumor 13 and the corresponding brain [lanes 14 and 15]). (C) DNAs from tumors 15, 16, 18, 14, 12, 5, 106-1, 106-2, 106-3, 105-1, and 3 (lanes 2 to 12, respectively). Lanes 1, DNA from normal NIH/Swiss liver.

contains a unique *Sac*I site in its LTR which allows precise localization of the insertion point. All tumors showed a 3.3-kbp fragment corresponding to the normal allele (Fig. 3B, lane 1) and a rearranged fragment of 2.2 kbp (lanes 2 to 12 and 14). Thus, the rearrangements in the *Sic-1* region appear to be the result of a proviral integration within a very small DNA region (100 bp or less, as defined by the limit of resolution of the gel electrophoresis analysis). However, even though all the rearranged *Sac*I fragments appear to be the same size, two integration clusters were defined according to the absence or presence of rearranged fragments in the *Pst*I-digested tumor DNAs (Fig. 3C). The two clusters are located immediately adjacent to a *Pst*I restriction endonuclease site in the genomic DNA (Fig. 4). Whether a given

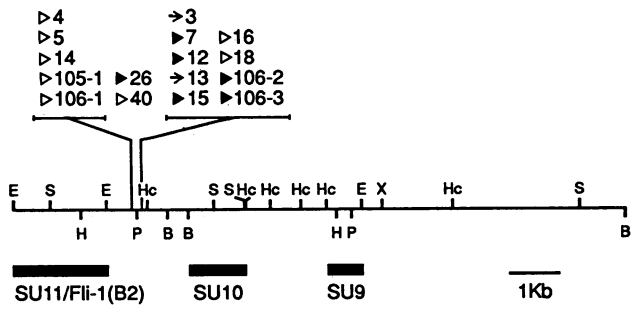

FIG. 4. Partial restriction endonuclease map and positions of viral integrations in the *Sic-1* region. Fourteen of the proviral integrations have been assigned to one of two clusters, both localized within less than 100 bp immediately 5′ or 3′ of the *Pst*I site as indicated. Integrations in tumors 26 and 40 lie in the same 100-bp region. The 5′-to-3′ orientations of ecotropic (▷), MCF-like (▶), and undetermined (→) proviruses are shown. Abbreviations for restriction endonucleases: B, *Bam*HI; E, *Eco*RI; H, *Hin*dIII; Hc, *Hin*cII; K, *Kpn*I; P, *Pst*I; S, *Sac*I; X, *Xba*I. The SU9, SU10, and SU11/*Fli-1*(B2) (3) probes are also shown (▬).

integration will lead to a *Pst*I rearrangement detectable with SU10 or not depends on its location either 3′ or 5′ of *Pst*I, respectively. Finally, the orientation of the proviruses was determined by digestion with *Hin*dIII or *Pst*I, which cleave the Cas-Br-E genome asymetrically. All proviruses are integrated in the same 5′-to-3′ orientation (Fig. 4).

Assignment of the *Sic-1* region to chromosome 9 and fine structure mapping. The mouse *Sic-1* region was initially mapped by the analysis of Chinese hamster-mouse somatic cell hybrids. Southern hybridization of *Sac*I-digested hybrid DNAs with the SU10 probe showed a unique 3.3-kbp fragment. Cross-reactive hybridization with *Sac*I-digested hamster DNA generated a smear. DNAs from 22 hybrid lines were examined for the presence or absence of the 3.3-kbp mouse fragment corresponding to SU10. Analyses of the chromosome contents of these hybrids showed that *Sic-1* maps to chromosome 9 (data not shown). To determine the map position of *Sic-1* on chromosome 9, segregation of *Sic-1* was compared with that of *Mpi-1* (mannose phosphate isomerase-1) and *Cbl-2*. *Mpi-1* was typed by histochemical staining of kidney extracts following electrophoresis on starch gels (19). *Cbl-2* was typed by Southern blot analysis with the v-*cbl* probe (47), which cross-hybridized with *Pvu*II 8.2-, 2.3-, and 1.4-kbp fragments in the parental NFS/N mouse DNA and 4.7-, 2.7-, 1.0-kbp fragments in *M. musculus*. The *Cbl-2* locus was scored by segregation of the 2.3- and 1.4-kbp NFS/N fragments, and *Cbl-1* on chromosome 6 was scored by segregation of the 8.2-kbp fragment. Hybridization with SU9 identified a 9.1-kbp *Sca*I fragment in *M. musculus* and a 21.0-kbp *Sca*I fragment in NFS/N. Examination of backcross progeny for these markers showed that the genes are linked with gene order: centromere–*Sic-1*–*Cbl-2*–*Mpi-1* (Table 2). These data position *Sic-1* in the centromeric region of chromosome 9 and establish that it is distinct from the proto-oncogene *Cbl-2*. However, these data also indicate that *Sic-1* maps near three other loci described as proto-oncogenes or common viral integration sites, *Ets-1*, *Tpl-1*, and *Fli-1*. Mouse genomic DNA was digested by several restriction enzymes and analyzed after Southern transfer with *Tpl-1*, *Ets-1*, and *Fli-1* probes, and the results were compared with those obtained with different probes spanning 30 kbp of the *Sic-1* DNA region. No correlation was observed in the size of the hybridized mouse DNA fragments between *Sic-1* and the *Tpl-1* and *Ets-1* probes. However, the hybridization pattern obtained with the *Fli-1* probe was indistinguishable from that obtained with the *Sic-1* probe SU11 (results not shown). Moreover, when DNAs of several Cas-Br-E-induced lymphomas were analyzed with the *Sic-1* and *Fli-1* probes, the two probes detected the same DNA rearrangements. Therefore, we conclude that *Sic-1* and *Fli-1* are identical and correspond to the same locus.

TABLE 1. Restriction enzyme analysis of the *Sic-1* region in Cas-Br-E MuLV-induced lymphomas[a]

Source of DNA	Type of proviral insertion	Latency (wk)	Fragment size (kbp) detected with *Sic-1*-specific probe after digestion with:			
			*Eco*RI	*Sac*I	*Pst*I	*Hin*dIII
Liver			5.0	3.3	4.3	5.0
Tumor[b]						
3	ND	14	ND	2.2	12.0	ND
4	Eco	12	13.8	2.2[c]	NR	7.3
5	Eco	12	13.8	2.2[c]	NR	7.3
7	Eco	16	13.8	2.2	12.0	ND
12	Eco	14	13.8	2.2	12.0	7.3
13	Eco/MCF[d]	14	13/8/6.0	2.2	12.0	7.3
14	Eco	14	13.8	2.2[c]	NR	7.3
15	MCF	14	6.0	2.2	12.0	ND
16	Eco	14	13.8	2.2	12.0	ND
18	Eco	16	13.8	2.2	12.0	ND
26	MCF	14	6.0	ND	ND	ND
40	Eco	18	13.8	ND	ND	7.3
105-1	Eco	53	13.8	2.2[c]	NR	7.3
106-1	Eco	26	13.8	2.2[c]	NR	ND
106-2	MCF	27	6.0	2.2	10.0	7.0
106-3	MCF	27	6.0	2.2	10.0	7.3

[a] Eco, Ecotropic virus; ND, not determined; NR, no rearrangements.
[b] In each tumor, the normal fragment seen in liver DNA was also detected.
[c] *Sac*I fragments (2.2 kbp), with integration upstream of the *Pst*I restriction site, indistinguishable from 2.2-kbp *Sac*I fragments, with integration downstream of *Pst*I. The difference between the two sites would be less than 100 bp. (Fig. 4).
[d] Tumor contains rearrangements corresponding to both types of insertion.

TABLE 2. Segregation of the *Sic-1* hybridizing restriction fragment with alleles of *Mpi-1* and *Cbl-2* in 59 progeny of an interspecies backcross

Marker	No. (%) of recombinants[a]:		
	Sic-1	*Cbl-2*	*Mpi-1*
Sic-1		4/59 (6.8 ± 3.3)	9/59 (15.3 ± 4.7)[b]
Cbl-2			5/59 (8.5 ± 3.6)

[a] Percent recombination between restriction fragments and standard errors were calculated by the method of Green (18) from the number of recombinants per total number of animals analyzed. Loci are listed in order with respect to the centromere.
[b] An additional 38 mice were typed only for *Sic-1* and *Mpi-1*, providing a total recombination of 18 of 97 (18.6% ± 4.0%).

DISCUSSION

Cas-Br-E MuLV is a useful virus for the detection of common viral integration sites in mouse tumors for two reasons. First, it induces different hematopoietic tumors in different mouse genetic backgrounds and therefore may help to identify a broader range of integration sites than other

MuLVs. Second, its sequence divergence from the endogenous proviral sequences present in laboratory strains permits segments of its genome to be used as hybridization probes. From the analysis of Cas-Br-E MuLV-induced non-T, non-B lymphomas, we found a high level of specific integration in a mouse DNA region that we called *Sic-1*. Indeed, the frequency of occupancy of the *Sic-1* region is very high (67% of the tumors analyzed) and significantly exceeds the frequency expected for random integrations. This finding is a strong indication that rearrangements in that region contribute to tumor initiation or progression.

Tumor induction by Cas-Br-E MuLV has been associated previously with two common integration sites: *Evi-1* (31) and *Myb* (65), located on mouse chromosomes 3 (31) and 10 (49), respectively. The *Sic-1* region, mapped to mouse chromosome 9, represents a third locus associated with the Cas-Br-E MuLV. *Sic-1* resides on the same chromosome as the proto-oncogenes *Cbl-2* (47) and *Ets-1* (27) and the common integration sites *Tpl-1* (2) and *Fli-1* (3). *Cbl-2* is related to a viral oncogene transduced following Cas-Br-E MuLV induction of a pre-B-cell lymphomas (29). This acute virus induces mainly pre-B-cell lymphomas and occasionally pro-B-cell and myeloid tumors. Despite their association with the same Cas-Br-E viral origin, *Sic-1* and *Cbl-2* represent two distinct loci, since they map to different portions of chromosome 9. The *ets* sequence was identified in the avian replication-defective retrovirus E26, which also contains the *myb* oncogene (63). Induction of erythroblastosis in chicken, in addition to myeloblastosis, is thought to be mediated by the unique *ets* sequence or by a cooperative effect of *myb* and *ets* (37). The *Tpl-1* region, highly homologous to *Ets-1*, has been shown to be commonly rearranged in the progression of rat T-cell lymphomas induced by Moloney MuLV (2). DNA rearrangements of the *Fli-1* region have been shown to occur in Friend MuLV-induced erythroleukemia (3). It has been suggested that *Fli-1* and *Ets-1* regions, localized within 0 to 2 centimorgans from each other, are distinct loci (3). In our genomic DNA mapping experiments, a comparison of hybridized restriction patterns indicates that at least the 30-kbp DNA region surrounding *Sic-1* does not overlap with *Ets-1* or *Tpl-1*. However, our data also clearly indicate that the *Sic-1* region is identical to the *Fli-1* locus. Even if that region is distinct from *Ets-1* and *Tpl-1*, proviral integration can still result in the *cis* activation of *Ets-1* and *Tpl-1* expression. Indeed, proviruses have recently been shown to activate a gene located as far as 270 kbp away from the integration site (57).

Perhaps the most striking feature in our Cas-Br-E MuLV-induced tumor system is that all ecotropic and MCF-like proviruses found linked to *Fli-1* (*Sic-1*) are clustered within a very small chromosomal area (16 integrations in less than 100 bp), and are identically oriented. This specificity suggests that the oncogenic effect of viral integration is subject to strict molecular constraints. Strong clustering of integration in a narrow area was observed for instance in activation of c-*erb-B* in avian-erythroleukemia due to viral promoter insertion (44) or in activation of N-*myc* in T-cell lymphoma, either by enhancer activity from the Moloney MuLV LTR or by removal of a negative element in the 3′ untranslated region or both (59). A similar narrow clustering was also reported in the Moloney MuLV integrations in the 3′ untranslated region of the *Pim-1* locus (51). By analogy, we believe that the Cas-Br-E integration into the *Fli-1* region could be closely associated with a transcribed region.

On the other hand, it has been reported that Cas-Br-E MuLV induces lymphomas with no classic T- or B-cell surface markers, suggesting that tumor cells could be of stem cell origin (5). The early stage of maturation of these cells is further suggested by our results showing that neither the immunoglobulin heavy chain gene nor the T-cell receptor β-chain gene is rearranged in tumor DNA. These target cells may represent immature cells already committed to lymphoid lineage but also common progenitors for different lineages. Cell surface markers and gene expression analysis will be necessary to better characterize these target cells. It is interesting that Friend MuLV integrations in *Fli-1* span a 2-kbp DNA region and are all in the opposite orientation when compared to Cas-Br-E provirus integration (3). Moreover, Ben-David et al. (3) have reported *Fli-1* DNA rearrangements exclusively in erythroleukemias, suggesting that different target cells, not necessarily from different lineages, seem to be implicated in these Cas-Br-E and Friend MuLV-induced tumors. These variations in the structural organization of Friend and Cas-Br-E proviruses in the *Fli-1* region suggest that molecular constraints differ in the two systems and may reflect the difference in target cells. Indeed, it has been shown that integration is not completely random (53), with proviruses preferentially integrating near DNase I-hypersensitive sites and transcriptionally active regions (48, 50, 61). This restriction could influence the accessibility to retrovirus integration. Alternatively, viral integration can affect normal gene expression by virtue of different mechanisms (8, 9, 31, 35, 36, 55, 64). Many factors including the intrinsic virus properties such as cell targeting, strength, and plurivalence of promoter or enhancer and possibly other viral sequences (25, 66) could affect the mechanism of tumor induction. In this particular case, it is possible that the difference observed between the proviral organization of Cas-Br-E MuLV and Friend MuLV in the *Fli-1* region reflects the utilization of two different mechanisms of oncogenic activation or even the activation of different genes. It is worth noting that the current mapping data place *Fli-1* in a large cluster of mouse genes whose human analogs have been mapped to chromosome 11 in a conserved arrangement (27, 34). This region of the human genome associated with various leukemias could be associated with several proto-oncogenes.

The analysis of Cas-Br-E MuLV integration in non-T-, non-B-cell lymphomas has successfully allowed the identification of a new murine common site of viral integration which is different from the two previously reported Cas-Br-E tumor-associated integration sites: *Evi-1* and *Myb*. This region may identify a new proto-oncogene. The fact that the *Fli-1* region is not occupied by a provirus in 100% of the tumors suggests that other genetic events have occurred in *Fli-1*-negative tumors. The analysis of such negative non-T-, non-B-cell lymphomas could be used to search for other potential proto-oncogenes activated by viral insertion.

ACKNOWLEDGMENTS

We gratefully acknowledge M. Maheu from Hôpital Notre Dame, Montréal, and J. P. Descoteaux from Institut Armand Frappier, Montréal, for their important contribution in pathological analysis; A. Bernstein and P. Tsichlis for providing the *Fli-1*, *Tpl-1*, and *Ets-1* probes; M. Ru and M. Sitbon for helpful discussions; R. Bergeron, Y. Bastien, and M. C. Adamson for excellent technical assistance; R. Milne for reviewing the manuscript; and L. Roy and B. Cloutier for preparation of the manuscript.

This work was supported by the Medical Research Council of Canada. D.B. was a fellow of the Société de Recherche sur le Cancer Inc. and the Fondation de l'Université du Québec à Montréal.

REFERENCES

1. **Alt, F. W., N. Rosenberg, R. J. Casanova, E. Thomas, and D. Baltimore.** 1982. Immunoglobulin heavy-chain expression and class switching in a murine leukaemia cell line. Nature (London) **296**:325–331.
2. **Bear, S. E., A. Bellacosa, P. A. Lazo, N. A. Jenkins, N. G. Copeland, H. Hanson, G. Levan, and P. N. Tsichlis.** 1989. Provirus insertion in *Tpl-1*, an *Ets-1* related oncogene, is associated with tumor progression in Moloney murine leukemia virus-induced rat thymic lymphomas. Proc. Natl. Acad. Sci. USA **86**:7495–7499.
3. **Ben-David, Y., E. B. Giddens, and A. Bernstein.** 1990. Identification and mapping of a common proviral integration site *Fli-1* in erythroleukemia cells induced by Friend murine leukemia virus. Proc. Natl. Acad. Sci. USA **87**:1332–1336.
4. **Breuer, G. L., H. T. Cuypers, and A. Berns.** 1989. Evidence for the involvement of *pim-2*, a new common proviral insertion site, in progression of lymphomas. EMBO J. **8**:743–747.
5. **Bryant, M. L., J. L. Scott, B. K. Pall, J. D. Estes, and M. B. Gardner.** 1981. Immunopathology of natural and experimental lymphomas induced by wild mouse leukemia virus. Am. J. Pathol. **104**:272–282.
6. **Caccia, N., M. Kronenberg, D. Saxe, R. Haars, G. A. P. Bruns, J. Governman, M. Malissen, H. Williard, Y. Yoshikai, M. Simon, L. Hood, and L. Mak.** 1984. The T cell receptor β chain genes are located on chromosome 6 in mice and chromosome 7 in humans. Cell **37**:1091–1099.
7. **Chattopadhyay, S. K., B. M. Baroudy, K. L. Holmes, T. N. Frederickson, M. R. Lander, H. C. Morse III, and J. W. Hartley.** 1989. Biologic and molecular genetic characteristics of a unique MCF virus that is highly leukemogenic in ecotropic virus-negative mice. Virology **168**:90–100.
8. **Corcoran, L. M., J. M. Adams, A. R. Dunn, and S. Cory.** 1984. Murine T lymphomas in which the cellular *myc* oncogene has been activated by retroviral insertion. Cell **37**:113–122.
9. **Cuypers, H. T., G. Selten, W. Quint, M. Zijlstra, E. R. Maandag, W. Boelens, P. Van Wezenbeck, C. Melief, and A. Berns.** 1984. Murine leukemia virus-induced T-cell lymphomagenesis: integration of proviruses in a distinct chromosomal region. Cell **37**:141–150.
10. **Dolcetti, R., S. Rizzo, A. Viel, R. Maestro, V. DeRe, G. Feriotto, and M. Boiocchi.** 1989. *N-myc* activation by proviral insertion in MCF 247 induced murine T-cell lymphomas. Oncogene **4**:1009–1014.
11. **Feinberg, A. P., and B. Vogelstein.** 1984. A technique for radiolabeling DNA restriction fragments to high specific activity. Anal. Biochem. **137**:266–267.
12. **Fredrickson, T. N., W. Y. Langdon, P. M. Hoffman, J. W. Hartley, and H. C. Morse III.** 1984. Histological and cell surface antigen studies of hematopoietic tumors induced by Cas-Br-M murine leukemia virus. J. Natl. Cancer Inst. **72**:447–454.
13. **Gallahan, D., C. Kozak, and R. Callahan.** 1987. A new common integration region (*int-3*) for mouse mammary tumor virus on mouse chromosome 17. J. Virol. **61**:218–220.
14. **Garcia, M., R. Wellinger, A. Vessaz, and H. Diggelmamm.** 1986. A new site of integration for mouse mammary tumor virus proviral DNA common to BALB/c (C3H) mammary and kidney adenocarcinomas. EMBO J. **5**:127–134.
15. **Gardner, M. B.** 1978. Type C viruses of wild mice: characterization and natural history of amphotropic, ecotropic and xenotropic murine leukemia viruses. Curr. Top. Microbiol. Immunol. **79**:215–239.
16. **Gardner, M. B., V. Klement, B. E. Henderson, J. Casagrande, M. L. Bryant, M. F. Dougherty, and J. D. Estes.** 1978. Lymphoma, paralysis and oncornaviruses of wild mice, p. 343–356. *In* L. Severi (ed.), Tumors of early life in man and animals. Perugia Quadrennial International Conference on Cancer. Monteluce, Italy.
17. **Gisselbrecht, S., S. Fichelson, B. Sola, D. Bordereaux, A. Hampe, C. Andre, F. Galibert, and P. Tambourin.** 1987. Frequent *c-fms* activation by proviral insertion in mouse myeloblastic leukaemias. Nature (Nature) **329**:259–261.
18. **Green, E. L.** 1981. Breeding system, p. 91–104. *In* H. L. Foster, J. D. Smith, and J. G. Fox. (ed.), The mouse in biomedical research, vol. 1. Academic Press, Inc., New York.
19. **Harris, H., and D. A. Hopkinson.** 1976. Handbook of enzyme electrophoresis in human genetics. Elsevier/North-Holland Publishing Co., Amsterdam.
20. **Hartley, J. W., and W. P. Rowe.** 1976. Naturally occurring murine leukemia viruses in wild mice: characterization of a new "amphotropic" class. J. Virol. **19**:19–25.
21. **Hoffman, P. M., W. F. Davidson, S. K. Ruscetti, T. M. Chused, and H. C. Morse III.** 1981. Wild mouse ecotropic murine leukemia virus infection of inbred mice: dual-tropic virus expression precedes the onset of paralysis and lymphoma. J. Virol. **39**:597–602.
22. **Hoggan, M. D., N. F. Halden, C. E. Buckler, and C. A. Kozak.** 1988. Genetic mapping of the mouse c-*fms* proto-oncogene to chromosome 18. J. Virol. **62**:1055–1056.
23. **Holmes, K., W. Y. Langdon, T. N. Fredrickson, R. L. Coffmann, P. M. Hoffman, J. W. Hartley, and H. C. Morse III.** 1986. Analysis of neoplasms induced by Cas-Br-M MuLV tumor extracts. J. Immunol. **137**:679–688.
24. **Ihle, J. N., B. Smith-White, B. Sisson, D. Parker, D. Blair, A. Schultz, C. Kozak, R. D. Lunsford, D. Askew, Y. Weinstein, and R. J. Isfort.** 1989. Activation of the c-H-*ras* proto-oncogene by retrovirus insertion and chromosomal rearrangement in a Moloney leukemia virus-induced T-cell leukemia. J. Virol. **63**:2959–2966.
25. **Jolicoeur, P., and L. Desgroseillers.** 1985. Neurotropic Cas-Br-E murine leukemia virus harbors several determinants of leukemogenicity mapping in different regions of the genome. J. Virol. **56**:639–643.
26. **Jolicoeur, P., N. Nicolaiew, L. Desgroseillers, and E. Rassart.** 1983. Molecular cloning of infectious viral DNA from ecotropic neurotropic wild mouse retrovirus. J. Virol. **45**:1159–1163.
27. **Kingsley, D. M., N. A. Jenkins, and N. E. Copeland.** 1989. A molecular genetic linkage map of mouse chromosome 9 with regional localizations for the *Gsta*, *T3q*, *Ets-1* and *Ldlr* loci. Genetics **123**:165–172.
28. **Koehne, C. F., P. A. Lazo, K. Alves, J. S. Lee, P. N. Tsichlis, and P. V. O'Donnell.** 1989. The *Mlvi-1* locus involved in the induction of rat T-cell lymphomas and the *pvt-1*/*Mis-1* locus are identical. J. Virol. **63**:2366–2369.
29. **Langdon, W. Y., J. M. Hartley, S. P. Klinken, S. K. Ruscetti, and H. C. Morse III.** 1989. *V-cbl*, an oncogene from a dual-recombinant murine retrovirus that induces early B-lineage lymphomas. Proc. Natl. Acad. Sci. USA **86**:1168–1172.
30. **Moreau-Gachelin, F., A. Tavitian, and P. Tambourin.** 1988. *Spi-1* is a putative oncogene in virally induced murine erythroleukaemias. Nature (London) **331**:277–279.
31. **Morishita, K., D. S. Parker, M. L. Mucenski, N. A. Jenkins, N. G. Copeland, and J. N. Ihle.** 1988. Retroviral activation of a novel gene encoding a zinc finger protein in IL-3-dependent myeloid leukemia cell lines. Cell **54**:831–840.
32. **Mucenski, M. L., D. J. Gilbert, B. A. Taylor, N. A. Jenkins, and N. G. Copeland.** 1987. Common sites of viral integration in lymphomas arising in AKXD recombinant inbred mouse strains. Oncogene Res. **2**:33–48.
33. **Mucenski, M. L., B. A. Taylor, J. N. Ihle, J. W. Hartley, H. C. Morse III, N. A. Jenkins, and N. G. Copeland.** 1988. Identification of a common ecotropic viral integration site, *Evi-1*, in the DNA of AKXD murine myeloid tumors. Mol. Cell. Biol. **8**:301–308.
34. **Nadeau, J. H.** 1989. Maps of linkage and synteny homologies between mouse and man. Trends Genet. **5**:82–86.
35. **Neel, B. G., W. S. Hayward, H. L. Robinson, J. Fang, and S. M. Astrin.** 1981. Avian leukosis virus-induced tumors have common proviral integration sites and synthesize discrete new RNAs: oncogenesis by promoter insertion. Cell **23**:323–334.
36. **Neil, J. C., and D. Forrest.** 1987. Mechanisms of retrovirus-induced leukemia: selected aspects. Biochim. Biophys. Acta **907**:71–91.
37. **Nunn, M. F., P. H. Seeberg, C. Moscovici, and P. H. Duesberg.** 1983. Tripartite structure of the avian erythroblastosis virus E26 transforming gene. Nature (London) **306**:391–395.

38. **Nusse, R., and H. E. Varmus.** 1982. Many tumors induced by the mouse mammary tumor virus contain a provirus integrated in the same region of the host genome. Cell **31**:99–109.
39. **Pattengale, P. K., and C. R. Taylor.** 1983. Experimental models of lymphoproliferative disease. The mouse as a model for human non-Hodgkin's lymphomas and related leukemias. Am. J. Pathol. **113**:235–265.
40. **Peters, G., A. I. Lee, and C. Dickson.** 1986. Concerted activation of two potential proto-oncogenes in carcinomas induced by mouse mammary tumour virus. Nature (London) **320**:628–631.
41. **Poirier, Y., and P. Jolicoeur.** 1989. Distinct helper virus requirements for Abelson murine leukemia virus-induced pre-B and T-cell lymphomas. J. Virol. **63**:2088–2098.
42. **Poirier, Y., C. Kozak, and P. Jolicoeur.** 1988. Identification of a common helper provirus integration site in Abelson murine leukemia virus-induced lymphoma DNA. J. Virol. **62**:3985–3992.
43. **Quint, W., W. Quax, H. Van Der Putten, and A. Berns.** 1981. Characterization of AKR murine leukemia sequences in AKR mouse substrains and structure of integrated recombinant genomes in tumor tissues. J. Virol. **39**:1–10.
44. **Raines, M. A., G. L. Wynne, W. G. Lewis, L. B. Crittenden, and H. J. Kung.** 1985. *c-erbB* activation in avian leukosis virus-induced erythroblastosis: clustered integration sites and the arrangement of provirus in the *c-erbB* alleles. Proc. Natl. Acad. Sci. USA **82**:2287–2291.
45. **Rassart, E., L. Desgroseillers, and P. Jolicoeur.** 1981. Molecular cloning of B- and N-tropic endogenous BALB/c murine leukemia virus circular DNA intermediates: isolation and characterization of infectious recombinant clones. J. Virol. **39**:162–171.
46. **Rassart, E., L. Nelbach, and P. Jolicoeur.** 1986. Cas-Br-E murine leukemia virus: sequencing of the paralytogenic region of its genome and derivation of specific probes to study the origin and structure of its recombinant genome in leukemic tissues. J. Virol. **60**:910–919.
47. **Regnier, D. C., C. A. Kozak, D. M. Kingsley, N. A. Jenkins, N. G. Copeland, W. Y. Langdon, and H. C. Morse III.** 1989. Identification of two murine loci homologous to the v-*cbl* oncogene. J. Virol. **63**:3678–3682.
48. **Rohdewohld, H., H. Weiher, W. Reik, R. Jaenisch, and M. Breindl.** 1987. Retrovirus integration and chromatin structure: Moloney murine leukemia proviral integration sites map near DNase I-hypersensitive sites. J. Virol. **61**:336–343.
49. **Sakaguchi, A. Y., P. A. Lalley, B. U. Zabel, R. W. Ellis, E. M. Scolnick, and S. L. Naylor.** 1984. Chromosome assignments of four mouse cellular homologs of sarcoma and leukemia oncogenes. Proc. Natl. Acad. Sci. USA **81**:525–529.
50. **Scherdin, U., K. Rhodes, and M. Breindl.** 1990. Transcriptionally active genome regions are preferred targets for retrovirus integration. J. Virol. **64**:907–912.
51. **Selten, G., H. T. Cuypers, W. Boelens, E. Robanus-Maandag, J. Verbeek, J. Domen, C. Van Beveren, and A. Berns.** 1986. The primary structure of the putative oncogene *pim-1* shows extensive homology with protein kinases. Cell **46**:603–611.
52. **Shen-Ong, G. L. C., and L. Wolff.** 1987. Moloney murine leukemia virus-induced myeloid tumors in adult BALB/c mice: requirement of c-*myb* activation but lack of v-*abl* involvement. J. Virol. **61**:3721–3725.
53. **Shih, C. C., J. P. Stoye, and J. M. Coffin.** 1988. Highly preferred targets for retrovirus integration. Cell **53**:531–537.
54. **Silver, J., and C. Kozak.** 1986. Common proviral integration region on a mouse chromosome 7 in lymphomas and myelogenous leukemias induced by Friend murine leukemia virus. J. Virol. **57**:526–533.
55. **Sola, B., S. Fichelson, D. Bordereaux, P. E. Tambourin, and S. Gisselbrecht.** 1986. *fim-1* and *fim-2*: two new integration regions of Friend murine leukemia virus in myeloblastic leukemias. J. Virol. **60**:718–725.
56. **Sola, B., D. Simon, M. G. Mattei, S. Fichelson, D. Bordereaux, P. E. Tambourin, J. L. Guenet, and S. Gisselbrecht.** 1988. *fim-1*, *fim-2*/c-*fms*, and *fim-3*, three common integration sites of Friend murine leukemia virus in myeloblastic leukemias map to mouse chromosomes 13, 18, and 3, respectively. J. Virol. **62**:3973–3978.
57. **Tsichlis, P. N., B. M. Shepherd, and S. E. Bear.** 1989. Activation of the *Mlvi-1*/*mis-1*/*pvt-1* locus in Moloney murine leukemia virus-induced T-cell lymphomas. Proc. Natl. Acad. Sci. USA **86**:5487–5491.
58. **Tsichlis, P. N., P. G. Strauss, and M. A. Lohse.** 1985. Concerted DNA rearrangements in Moloney murine leukemia virus-induced thymomas: a potential synergistic relationship in oncogenesis. J. Virol. **56**:258–267.
59. **Van Lohuizen, M., M. Breuer, and A. Berns.** 1989. *N-myc* is frequently activated by proviral insertion in MuLV-induced T-cell lymphomas. EMBO J. **8**:133–136.
60. **Vijaya, S., D. L. Steffen, C. Kozak, and H. L. Robinson.** 1987. *dsi-1*, a region with frequent proviral insertions in Moloney murine leukemia virus-induced rat thymomas. J. Virol. **61**:1164–1170.
61. **Vijaya, S., D. L. Steffen, and H. L. Robinson.** 1986. Acceptor sites for retroviral integrations map near DNase I-hypersensitive sites in chromatin. J. Virol. **60**:683–692.
62. **Villemur, R., Y. Monczak, E. Rassart, C. Kozak, and P. Jolicoeur.** 1987. Identification of a new common provirus integration site in Gross passage A murine leukemia virus-induced mouse thymoma DNA. Mol. Cell. Biol. **7**:512–522.
63. **Watson, D. K., M. J. McWilliams-Smith, C. Kozak, R. Reeves, J. Gearhart, M. F. Numm, W. Nash, J. R. Fowles III, P. Duesberg, T. S. Papas, and S. J. O'Brien.** 1986. Conserved chromosomal positions of dual domains of the *ets* protooncogene in cats, mice and humans. Proc. Natl. Acad. Sci. USA **83**:1792–1796.
64. **Weinstein, Y., J. L. Cleveland, D. S. Askew, U. R. Rapp, and J. N. Ihle.** 1987. Insertion and truncation of c-*myb* by murine leukemia virus in a myeloid cell line derived from cultures of normal hematopoietic cells. J. Virol. **61**:2339–2343.
65. **Weinstein, Y., J. N. Ihle, S. Lavu, and E. P. Reddy.** 1986. Truncation of the *c-myb* gene by a retroviral integration in an interleukin 3-dependent myeloid leukemia cell line. Proc. Natl. Acad. Sci. USA **83**:5010–5014.
66. **Wolff, L., and R. Koller.** 1990. Regions of the Moloney murine leukemia virus genome specifically related to induction of promonocytic tumors. J. Virol. **64**:155–160.